High-pressure x-ray scattering of oxides with a nanoscale local structure: Application to $Na_{1/2}Bi_{1/2}TiO_3$

J. Kreisel,[1,*] P. Bouvier,[2] B. Dkhil,[3] P. A. Thomas,[4] A. M. Glazer,[5] T. R. Welberry,[6] B. Chaabane,[1,2] and M. Mezouar[7]
[1]*Laboratoire Matériaux et Génie Physique, ENS de Physique de Grenoble, Boîte Postal 46, 38402 St. Martin d'Hères, France*
[2]*Laboratoire d'Electrochimie et de Physicochimie des Matériaux et des Interfaces, ENSEEG, Boîte Postal 75, 38402 St. Martin d'Hères Cedex, France*
[3]*Laboratoire Structures, Propriétés et Modélisation des Solides, Ecole Centrale Paris, 92290 Châtenay-Malabry, France*
[4]*Department of Physics, University of Warwick, Coventry CV4 7AL, United Kingdom*
[5]*Clarendon Laboratory, University of Oxford, Parks Road, Oxford OX1 3PU, United Kingdom*
[6]*Research School of Chemistry, Australian National University, Canberra ACT 0200, Australia*
[7]*European Synchrotron Radiation Facility (ESRF), Boîte Postal 220, 38043 Grenoble Cedex, France*
(Received 13 January 2003; published 29 July 2003)

Many of the outstanding properties in oxides are related to materials with an intrinsic nanoscaled local structure, where the different regions are characterized by competing chemical, structural, and/or physical properties. One of the major challenges in the analysis of the nanoscaled oxides is experimental access to the local properties, which is often at best a difficult task, a fact that often inhibits the understanding of properties such as colossal magnetoresistance, giant piezoelectricity, and high-temperature superconductivity. Here we present an investigation of the relaxor ferroelectric $Na_{1/2}Bi_{1/2}TiO_3$, considered as a model type of nanostructured oxide, by combining the parameter high-pressure with x-ray diffuse scattering. We show that nanoscaled characteristics can be investigated in detail by combining such measurements with simulation of different diffuse scattering models. We observe two distinct structural disorders, one of which is characterized by the observation of asymmetric diffuse scattering in perovskites due to planar polar defects.

DOI: 10.1103/PhysRevB.68.014113 PACS number(s): 61.10.Eq, 77.80.Bh, 64.70.Nd, 77.84.Dy

I. INTRODUCTION

The presence of a nanoscale structure is characteristic of so-called relaxor ferroelectrics (relaxors),[1] materials that have attracted considerable attention since the recent discovery of ultrahigh strain and giant piezoelectric properties in relaxor-based single crystals.[2,3] For another class of materials, namely, rare-earth manganite-based oxides displaying a giant magnetoresistance, the presence of nanoscaled phase separation features has been controversial, and it is only recently that this property has generally been accepted to be an intrinsic key feature.[4–9] Without being exhaustive, we mention in this connection high-T_c superconductors or more general correlated electron systems, which also display local intrinsic inhomogeneities.[4,10] On the way towards a fundamental understanding of nanoscaled materials, good knowledge of the local chemistry and structural properties is an important building block for the efficient and meaningful use of first principles *ab initio* calculations.[11–13] In addition, the understanding and tuning of local properties are of importance in creating new functional oxides with superior properties. Consequently, new approaches towards the detailed characterization of nanostructured materials are of interest. In the past, the usual approach towards the understanding of nanoscaled materials was mainly through their chemical composition- or temperature-dependent behavior. However, very recent high-pressure (>1.5 GPa) investigations of relaxor ferroelectrics[14,15] and manganite-type oxides[16,17] have illustrated the usefulness of pressure as a variable. We will illustrate in the following, that the combination of high pressure with (experimental and theoretical) x-ray diffuse scattering studies (XRDS) can lead to a deeper understanding of the physics and chemistry in nanoscaled materials.

II. EXPERIMENT

The system investigated in this work was the rhombohedral perovskite $Na_{1/2}Bi_{1/2}TiO_3$ (NBT), which is an example of a relaxor ferroelectric. NBT-based piezoelectrics offer exceptionally high strain and are thus a promising environmentally friendly alternative to the more usual toxic lead oxides.[18] NBT is unusual amongst perovskite materials since it appears to have an exact 1:1 ratio of two different cations Na and Bi in the *A* sites. The two cations have different charges and electronic configurations, but they possess similar ionic radii. The NBT single crystals used in the present work were prepared by the flux growth technique.[19,20] High-pressure XRDS experiments were performed at the European Synchrotron Radiation Facility (ESRF) at the ID30 high-pressure beam line. X-ray diffraction patterns, using the rotating crystal technique, were collected on a CCD detector (Bruker) with a focused monochromatic beam at wavelength $\lambda = 0.3738$ Å. The sample to detector distance and the CCD inclination angles were precisely calibrated using a silicon standard. High-pressure experiments on a crystal of 50 μm in size were performed with the focused beam on a diamond anvil cell with a 4:1 methanol:ethanol mixture as the pressure transmitting medium.

III. SCATTERING AT AMBIENT PRESSURE

Before discussing the x-ray scattering of NBT at different hydrostatic pressures it is useful to inspect the patterns at low

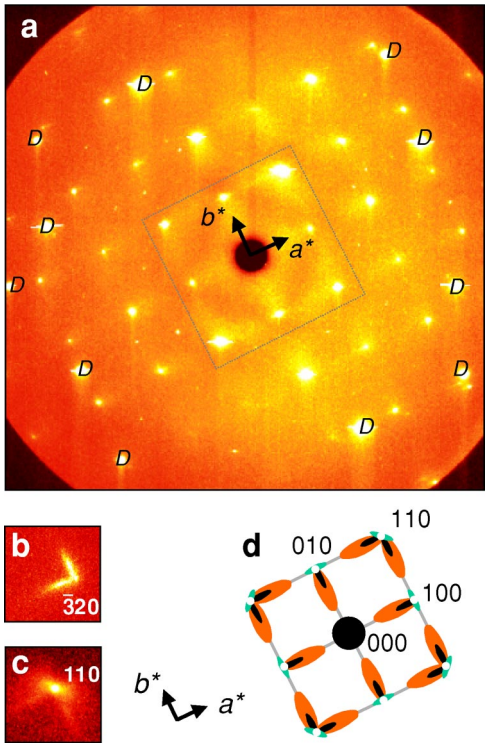

FIG. 1. (Color online) X-ray scattering imaging pattern for $Na_{1/2}Bi_{1/2}TiO_3$ at a hydrostatic pressure of 0.6 GPa, exhibiting the Bragg peaks from the average structure together with strong diffuse scattering originating from the nano-scaled structure. The sharp horizontal lines are due to the saturation of the detector. Spots denoted D are from the diamond anvil cell. To produce the pattern (a) the crystal was oscillated from $-15°$ to $+15°$, with respect to the incoming monochromatic synchrotron beam ($\lambda = 0.3738$ Å). Patterns (b)–(d) were obtained from small 0.5° oscillations around the Bragg angle of particular reflections to emphasize the diffuse scattering. (b) Pronounced asymmetric diffuse scattering around the $3\bar{2}0$ reflection. (c) Illustration of the superimposition of asymmetric scattering [black in part (d)] thermal scattering (green) and the large underlying scattering (orange), exemplified for the $1\bar{1}0$ reflection. (d) Schematic representation of the diffuse scattering in the dotted area of part (a) illustrating the superposition and direction of the diffuse scattering as exemplified in (b) and (c).

pressure. Figure 1 shows an example of an x-ray pattern from NBT exhibiting Bragg peaks, corresponding to the average crystal structure, together with diffuse scattering x-ray scattering. XRDS provides information on the deviations from the average structure and has been shown to be a well-adapted probe for the investigation of nanoscaled structural features.[21–24] Regarding the average structure, we observe, as in previous diffraction results,[19] a slight rhombohedral broadening of Bragg diffraction peaks and weak 311 superstructure[25] reflections. This phase of NBT is known to be rhombohedral with space group $R3c$.[19] The average structure is one in which the cations are displaced along [111] and the oxygen octahedra are tilted according to the tilt system $a^-a^-a^-$ (Glazer notation[26]).

The diffuse scattering occurs in two forms. (A) Sharp streaks emanating from Bragg peaks and extending along ⟨100⟩ directions [Fig. 1(b)]. These systematically appear only on the low-angle side of the Bragg peaks and for this reason we refer to these as asymmetric "L-shaped" peaks. Although asymmetric diffuse scattering is in itself not uncommon, we believe that this is the first time it has been reported in the important class of perovskites. (B) Rather broad diffuse regions of scattering most evident around the origin. In particular note the area confined within the diamond-shaped region bounded by lines joining the reciprocal lattice points 100, $0\bar{1}0$, $\bar{1}00$, 010.

In order to explain feature (A), it is necessary to assume some kind of planar defect (in 3D) reminiscent of Guinier-Preston zones (GPZ's), as seen in metal alloys such as AlCu solid solutions.[27] Such planar defects give rise to rods of diffuse scattering in reciprocal space, in directions normal to the planes of the defects. The marked asymmetry of the intensity of these rods with respect to the Bragg peak positions can be understood in terms of the so-called "atomic size-effect."[28–30] The asymmetry in the intensity results from the deformation of the structure around the chemical segregation planes.[27] It is thus tempting to invoke a similar explanation for the diffuse scattering from NBT. We should point out that an explanation purely and simply in terms of "atomic size" cannot hold for the case of NBT since Na^{1+} and Bi^{3+} have almost the same ionic radii: 0.97 and 0.96 Å, respectively. However, bond-valence calculations[31] show that in the average structure Bi is grossly underbonded while Na is somewhat overbonded. An observed "size-effect" might well be due to the excess charges on neighboring Bi ions causing the atoms to move further apart or alternatively to distort the structure in such a way that more of the negatively charged O^- ions are drawn into the space between them. Before presenting different models that can explain the observed pattern we will discuss in the following a structural view of NBT.

We assume that the principal structural elements responsible for the diffuse scattering will be associated with the Na and Bi parts of the structure. The average structure of the crystal can be thought of as consisting of unit cells in which the Na site is randomly occupied by Bi on a 1:1 basis, so that the average unit cell contains 0.5 Na superimposed on 0.5 Bi. As the space group is $R3c$, the structure is polar with average cation displacements along [111]. There is some evidence from x-ray and neutron diffraction experiments that the Bi shows larger polar displacements than for Na.[19,20,31] Furthermore, from a single-crystal diffraction experiment, it was found that the Bi shows an anomalously large isotropic displacement parameter. This is consistent with a model in which the Bi's are disordered about the average [111] direction, having small components of displacement perpendicular. Similar behavior has been noted for the Pb atom in PZT and PMN.[32,33] If Bi moves off the [111] axis towards any of the ⟨001⟩ directions, the effect is to reduce the local symmetry to monoclinic whereas the average symmetry remains rhombohedral (similar to the proposed model for lead-based relaxors[33]). The requirement for Bi to improve its coordination environment is seen as the main impetus for the deviations from the average structure that gives rise to the diffuse scattering. If regions within the crystal containing correlated ⟨001⟩ displacement components form, they can act as tem-

plates for the formation of the tetragonal phase in NBT and NBT-related systems on going to higher temperature.[19,20] The space group corresponding to the monoclinic structure might well be *Cm* the same as is found in the rhombohedral to tetragonal change with composition in $PbZr_xTi_{1-x}O_3$, but this will need further investigation.

Diffuse scattering arises from local departures from the average structure. In interpreting the diffuse scattering, we start by assuming that the majority of the NBT crystal has the average structure described above. We shall refer to this as the ''matrix.'' But how should we imagine the local deviations from this matrix, especially the structure, physics and chemistry behind the Guinier-Preston zones? Let us remember that the sharp asymmetric diffuse scattering originates from and is proportional to the difference $(F_{GPZ}-F_{matrix})^2$, of the structure factors due to the cations inside (F_{GPZ}) and outside (F_{matrix}) the GPZ zone. Such a difference can in principle come from a chemical and/or a structural difference and we thus suggest in this preliminary study two models that might well explain the observation of the well-defined asymmetric scattering (type A).

(1) The first model consists in assuming that the scatterers are different in the matrix and the GPZ, i.e., the GPZ consists of chemical segregation zones, for instance GPZ's rich in Bi and/or Na. Following the traditional idea of GPZ's the asymmetric scattering can then be explained by a correlation of the substitution-disorder (segregation) with a displacement-type disorder giving rise to a local deformation of the structure around the segregation planes.[27] The observed stronger diffuse scattering towards smaller angles is then explained by assuming that Bi^{3+} cations (which have larger scattering amplitude than the sodium) cause a local expansion of the structure around the GPZ. Alternatively if the GPZ's are rich in Na then the asymmetry can be explained by assuming that there is a local contraction of the structure. The latter model gains some support from the fact that Raman measurements have shown that at least some Na segregation exists in NBT.[34]

(2) The second model consists in considering that the two scatterers, inside and outside the GPZ, are on average chemically the same. That is, there is no chemical segregation but there is a structural origin shift within the GPZ, which leads to the observed scattering phenomenon. We consider that within the random matrix of rhombohedral symmetry the GPZ's are small planar islands of monoclinic symmetry, in which there are correlated displacements of Na's and Bi's with components parallel to the $\langle 001\rangle$ directions. Within these islands, there is still a random compositional arrangement of Na and Bi. The important difference between an island and the matrix is the direction of the displacements. In order to form the diffuse streaks, these islands must be predominantly in the form of small platelets oriented randomly perpendicular to all $\langle 001\rangle$ crystallographic directions throughout the matrix. Furthermore, in order for the scattering to be asymmetrically disposed around the Bragg peaks, it is also necessary for these islands to generate a ''size-effect'' strain such that the unit cells in the GPZ's are contracted in a direction perpendicular to the Na/Bi displacements. Note that both models have polar zones in a somewhat different matrix, which would then explain the observed relaxor-type dielectric properties.

IV. CALCULATION OF DIFFUSE SCATTERING

In order to try to establish the nature of the nano-scale structural features that give rise to the observed diffraction features in NBT we have carried out calculations using Monte Carlo (MC) simulation of some simple models, from which we calculated diffraction patterns for comparison to the observations. We have previously used such methods with success to aid in the interpretation and analysis of a wide variety of different disordered materials from ceramic oxides,[35,36] inclusion compounds,[37,38] inorganic and organometallic compounds,[39,40] pure organic molecular crystals,[41] and quasicrystals.[42]

For the present case of NBT we have used, for simplicity, only a two-dimensional (2D) model with which we represent the (001) projection of the structure. For this preliminary study we concentrate solely on the distribution of *A* cations since it is on these *A* sites that we expect to have Na/Bi substitutional disorder while the *B* cation sites and the oxygen anion arrays are expected to be essentially ordered. This simplification necessarily precludes any meaningful description of thermal diffuse scattering (TDS), which we would expect to be present in the system, and we have not attempted at this stage to include such effects in a model. Numerous variations of the two basic models (A) and (B) were investigated and full details of these investigations will be presented elsewhere. For the present purposes we show some selected results which demonstrate how the different diffraction features observed in NBT might arise.

In Fig. 2(a) we show a plot representing a small section (approximately 5%) of the distribution of *A* cations in a model crystal. The actual model used in the present work comprised 512×512 sites. Each pixel in Fig. 2(a) corresponds to a single site of the model lattice. A white square corresponds to occupancy by a Na atom and a gray square to occupancy by a Bi atom. The black squares, represent the GPZ defects which occur as linear features normal to [1 0] and [0 1]. In this example the GPZ was 2 unit cells wide but similar models with widths of 1 or 3 cells were also investigated. The three different diffraction patterns that are shown in Figs. 2(b)–2(d) were each computed from the same basic distribution shown in Fig. 2(a), but they differ in terms of exact details of what the GPZ's are comprised. For all three patterns the size-effect distortion applied used the same set of size-effect parameters. The mean length of neighboring Na-Na vectors was reduced by $\sim 2-3\%$ from the average while the mean length of neighboring Bi-Bi vectors was correspondingly increased by $\sim 2-3\%$. Na-Bi vectors were assumed to remain at the average value. Regarding the distortion around the GPZ's themselves, Na-GPZ, Bi-GPZ, and GPZ-GPZ vectors were reduced by $\sim 2-3\%$ from the average.

The model also includes Na/Bi occupancy disorder in the matrix part of the structure which results in the second type of diffuse scattering (form *B* above). This scattering, though very broad, tends to be concentrated around positions be-

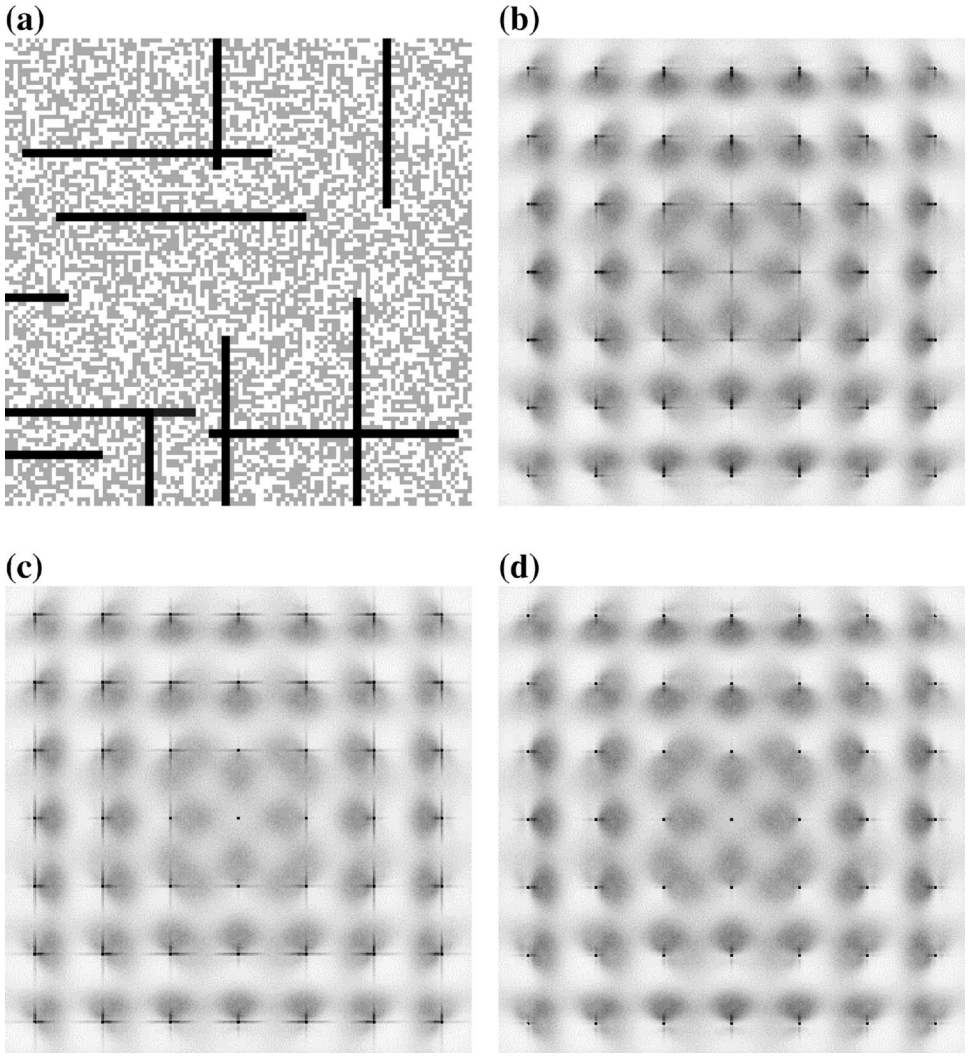

FIG. 2. Part (a) shows a small representative region of the model structure. White pixels represent unit cells containing Na, gray pixels cells unit cells containing Bi and black pixels represent GPZ's the nature of which are interpreted differently in making the calculations of the diffraction patterns in (b)–(d). In (b) the GPZ's are assumed to contain Na atoms. In (c) the GPZ's are assumed to have a scattering power equal to the average scattering power of the matrix, but these are displaced from the lattice site in a direction parallel to the length of the GPZ. (d) is the same as (c) but the magnitude of the displacement has been reduced to zero.

tween reciprocal lattice nodes and therefore indicates some local short-range order (SRO). The degree of SRO in Fig. 2(a) is in fact very small (Warren-Cowley SRO parameters in the $\langle 10 \rangle$ and $\langle 11 \rangle$ directions were 0.0 and -0.1, respectively) but is significantly different from a purely random distribution. These SRO parameters reflect a small tendency for alternate short rows of Bi- and Na-containing unit cells to occur in directions normal to each $\langle 100 \rangle$ direction. In considering the relaxor properties of NBT, this form of short-range order is of minor importance, compared with the presence of the GPZ's on the nanoscale, though it may indicate a tendency to reduce charge imbalance in the bulk of the lattice.

For Fig. 2(b) the atomic scattering factor for the GPZ sites was assumed to be Na and was located at the average site position. In this case the GPZ has an average scattering factor less than that of the disordered matrix. It should be noted that a diffraction pattern practically identical to that of Fig. 2(b) is obtained if the GPZ's are assumed to be Bi and at the same time the sign of the size-effect parameters for Na-GPZ, Bi-GPZ, and GPZ-GPZ is reversed, i.e., if the GPZs are Bi rich the distortion must correspond to an expansion of the lattice spacing around the GPZ's.

For Fig. 2(c) the atomic scattering factor of the GPZ sites was assumed to be the same as the average atomic scattering factor of the matrix. (This was in fact achieved using the atomic scattering factor for Ag, which comes midway between Bi and Na in the periodic table.) That there is now no contrast between the GPZ and the matrix is indicated by the fact that there is no cross at the center of the pattern. For Fig. 2(c), however, all the cations within the GPZ have been displaced in a direction parallel to the length of the GPZ, i.e., along $\langle 100 \rangle$. The quantity $(F_{\mathrm{GPZ}}-F_{\mathrm{matrix}})^2$ now becomes nonzero away from the origin of reciprocal space and the "*L*" shaped diffraction features can be seen again at higher angles. In contrast to Fig. 2(b) it is clear that this model

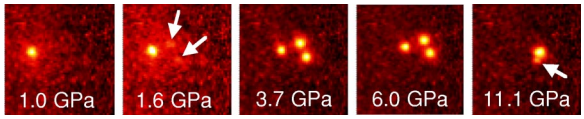

FIG. 3. (Color online) Images illustrating the pressure-dependent changes of the average structure for $Na_{1/2}Bi_{1/2}TiO_3$ exemplified by the behavior of the 300 reflection. The first transition is shown by a splitting of $\{h00\}$ reflections into three reflections, illustrating the crossover from a rhombohedral to a monoclinic (or lower symmetry) distortion. The observation of {310} and {210} superstructure reflections (not shown) in the monoclinic phase suggests a structure with in-phase octahedral tilts plus antiparallel cation displacements. Note that the 1.6 GPa pattern indicates a regime of rhombohedral-monoclinic phase coexistence. From 11.1 GPa onwards a new phase is observed through the change to a small tetragonal splitting. The distortion from the nearly metrically cubic structure is further shown by new {h odd 0} and {odd 0 0}.

results in the intensity of the L at the 320 reflection being greater than that at the 110 reflection.

In the final pattern, Fig. 2(d), all aspects of the calculation were the same as for Fig. 2(c) except that the displacement of the GPZ cations used for Fig. 2(c) has been reduced to zero. This demonstrates that if the effect of pressure on the model was to force the cations back toward the center of their coordination polyhedra (or to a correlated displacement value which is the same for the whole sample) then the L-shaped scattering would be expected to disappear. This would not be the case for the chemical segregation model of Fig. 2(b). It can be seen that Fig. 2(c) successfully models the observed XRDS features shown in Fig. 1.

From an experimental point of view, a low-angle scattering experiment could provide more evidence to determine whether chemical segregation exists or not. Finally, in our simulations we have found that the GPZ platelets need only be one or two unit cells thick to give the observed streak lengths, but the streak widths mean that lateral dimensions of the GPZ's must be of the order of 20 nm.

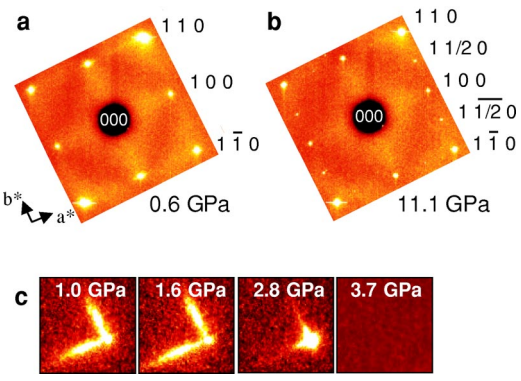

FIG. 4. (Color online) Pressure-dependent evolution of the diffuse scattering in NBT. (a), (b) Illustration of the pressure-independence of the diffuse scattering named type B in the text. Note, that the 11.1 GPa pattern is characterized by, first, the appearance of distortion-related superstructure reflections and second, a sharpening of the Bragg spots. The reduction of the asymmetric diffuse scattering around the $3\bar{2}0$ reflection in (c) gives evidence for fundamental structural changes on a local scale. Pattern c is obtained from small 0.5° oscillations around the Bragg angle of the $3\bar{2}0$ reflection to emphasize the diffuse scattering.

The occurrence of GPZ's with correlated cation displacements is important and, in particular, allows a new view of the temperature-dependent behavior of NBT, which undergoes two reversible phase transitions with decreasing temperature from the cubic prototypic phase ($Pm\bar{3}m$), to a tetragonal phase ($P4bm$) to the room-temperature rhombohedral $R3c$ phase.[19] The tetragonal-rhombohedral transition requires a radical rearrangement of the octahedral tilts from $a^0a^0c^+$ to $a^-a^-a^-$ and a redirection of the average cation displacements from [001] to [111].[19] The structural transformation is so drastic that at first sight it seems difficult to imagine how such a reversible change can be accomplished. The phase transition occurs sluggishly with a coexistence of the two phases over a considerable temperature interval. The local structure present in the rhombohedral phase can be seen to recall the nature of this phase transition. We can postulate that there is a competition between the tendency for rhombohedral ordering of the Ti-O framework with displacements along ⟨111⟩ and tetragonal Na/Bi displacements along ⟨001⟩. The final structure attained below the phase transition temperature possesses rhombohedral structure on average but retains some elements of the ⟨001⟩ displacements on the Na/Bi sites, as shown both by the Bi disorder in the matrix and the correlated displacements that give rise to the GPZ's. We believe that it is the existence of local monoclinic unit cells in the random matrix that provides a mechanism for the transformation. This is similar to recent models explaining the structure and remarkable piezoelectricity in lead-containing perovskite solid solutions at the so-called morphotropic phase boundary.[32,33]

V. THE EFFECT OF HIGH PRESSURE

The analysis of the diffraction pattern as a function of pressure illustrates that the average structure undergoes a rhombohedral-to-monoclinic transition between 1.6 and 2.0 GPa and then an monoclinic-to-tetragonal transition between 9.9 and 11.1 GPa (Fig. 3). The first phase transition is in agreement with diffraction investigations on powder samples[43] and in fact proceeds through a domain of coexistence, as can be seen by the incoming weak reflections at 1.6 GPa which attain full intensity at 2.0 GPa.

Further instructive information on the pressure-dependent behavior can be gained from the XRDS (Fig. 4). First of all, the form B diffuse scattering does not change with pressure [Figs. 4(a) and 4(b)], showing that there is no effective change in the Na-Bi short-range order, as expected since cation diffusion under high pressure is unlikely in the close-packed perovskite structure. Secondly, as the pressure increases up to 2.8 GPa the form A asymmetric XRDS around the Bragg spots loses much of its intensity [Fig. 4(c)] but only disappears at 3.7 GPa. The loss of form A scattering with pressure is consistent with a model where the matrix and the GPZ's adopt the same polar displacement (along [110] in the monoclinic phase) which then effectively suppresses the difference (thus deformation) between the matrix

and the GPZ's. Since high-pressure Raman spectroscopy[15] has revealed a pressure-induced suppression of the polar Ti^{4+} displacement, we might argue that the above outlined competition between a rhombohedral [111] and a tetragonal Na/Bi [001] displacement no longer exists, and this facilitates the development of a new long-range structure.

From the pressure dependent behavior it becomes clear that NBT is characterized by a local competition between different structures. In this sense we should mention that birefringence imaging[44] has shown that the rhombohedral phase rarely forms an optically homogeneous crystal, but consists of many regions with different orientations, where the slow axis direction tends to be closer to ⟨001⟩ directions, instead of the ⟨111⟩ directions required by rhombohedral symmetry. Since birefringence is a macroscopic quantity this can only be explained by an additional macroscopic strain within the NBT crystal, the origin of which was unknown until now. We can now suggest, that the accumulated strains caused by the presence of GPZ's (approximately 20 nm across) result in an optical strain that could even dominate the optical behavior due to the average structure.

It should be noted that the x-ray diffusion experiment described here has the invaluable advantage of yielding simultaneously information both about the average structure (via diffraction) and local deviations (via XRDS). This advantage allows us to address the frequent controversy concerning whether the difference in critical phase transition pressures, as measured by techniques with different characteristic spatial scales, such as Raman scattering and x-ray/neutron diffraction, for example, is intrinsic or not. Considering NBT, the critical pressures determined from high-pressure powder diffraction[43] and high-pressure Raman measurements[15] did not give the same information about the critical pressures for structural changes within the sample. As expected, the powder diffraction data gave correct evidence for a structural phase transition from rhombohedral to monoclinic (or possibly orthorhombic) symmetry at 1.6 to 2.0 GPa. However, the pressure-evolution of Raman bands suggested a further transition around 4.5 GPa, which was not registered in the powder diffraction data. The present study now shows that NBT undergoes in the pressure range up to 5 GPa two phase transitions occurring at different pressures: first, the crystallographic structural phase transition producing the change in long-range order from rhombohedral-to-monoclinic symmetry and second, a phase transition in the short-range order associated with the GPZ's. It is the use of the parameter high-pressure, implying important volume changes and thus major modifications of the energetic balance between long-range and different short-range order, which allows an easier (compared to temperature) discrimination of the characteristic features in relaxors and, more generally, in nanoscaled oxides.

VI. FINAL REMARKS

It should be reiterated that the achievement of a detailed knowledge of the average and local structure in a relaxor, together with its correlated or decorrelated nature, is by no means straightforward. For instance, there is still an open controversy concerning whether all relaxors are similar from a microstructural point of view or not. In this context let us consider the diffuse scattering of the two model relaxor ferroelectrics $PbMg_{1/3}Nb_{2/3}O_3$ and $Na_{1/2}Bi_{1/2}TiO_3$, which are often considered similar.[45] It is evident that the diffuse scattering patterns are distinctly different: the diffuse scattering is symmetric in PMN but asymmetric in NBT. This illustrates nicely, even without a deeper analysis, that these two relaxors should be different from a nanostructural point of view. Also, it is common consensus that the typical dielectric properties of relaxors originate in local polar zones, which are different from the rest of the matrix. However, the remaining question is whether these polar zones are associated with chemical ordering or not: in PMN, for example, such a link is usually accepted, even though it has not been demonstrated directly. Our present work shows that in NBT at least, the local Na-Bi ordering and the polar zones (GPZ's) are actually decorrelated. Therefore, combining these observations, we conclude that the local (polar and chemical) structure is very likely to be different from one relaxor to the other, which provides a new perspective for interpreting the differing properties observed in different relaxor systems. The corollary of this is that we dispense with the idea that relaxor properties are the consequence of a universal nanostructure common to all systems. While there is commonality in the nanostructure through the presence of polar zones, the details of the zones vary with those of the particular system in question. In NBT, for example, the crystallographic site that is shared is the *A* site of the perovskite structure upon which aliovalent ions (differing by 2) of the same size are substituted. By contrast, in PMN, the site-sharing is on the *B* site, with Mg and Nb both of different valence (by 3) and different size. The average symmetry in PMN is cubic and nonpolar whereas that in NBT is rhombohedral and polar, with the phase itself exhibiting ferroelectricity. All of these differences are expected to impact upon the details of the nanoscale structure as revealed by the diffuse scattering. What is also clear from this study is that high-pressure x-ray diffraction studies, particularly those in which Bragg peaks and diffuse scattering are simultaneously collected, present a powerful means for elucidating the broad similarities and detailed differences between the nanostructures of different relaxors. The technique is widely applicable to any nanostructured oxide for which a single-crystal sample of size 10 microns or above is available.

Finally, a good knowledge of the local structure, as provided by this study, is an important building block for first-principle calculations of relaxor ferroelectrics (and other nanostructured oxides). In the past, the use of the parameter high-pressure in first principle calculations was limited to classical ferroelectrics, for which it was shown to be very instructive (e.g., Refs. 46, 47). We believe that calculations of relaxors, as for instance presented in Refs. 11–13, combined with the parameter high-pressure will lead to further insight into relaxor physics. This study, together with high-pressure Raman studies on NBT and PMN (Refs. 14, 15) and very recent high-pressure diffuse scattering investigations of PMN,[48] provides the experimental basis for such investigations.

*Author to whom correspondence should be addressed. E-mail address: jens.kreisel@inpg.fr

[1] L. E. Cross, Ferroelectrics **76**, 241 (1987).
[2] S. E. Park and T. R. Shrout, J. Appl. Phys. **82**, 1804 (1997).
[3] H. Fu and R. E. Cohen, Nature (London) **403**, 281 (2000).
[4] J. Burgy, M. Mayr, V. Martin-Mayor, A. Moreo, and E. Dagotto, Phys. Rev. Lett. **87**, 277202 (2001).
[5] M. B. Bibes, L. Balcells, S. Valencia, J. Fontcuberta, M. Wojcik, E. Jedryka, and S. Nadolski, Phys. Rev. Lett. **87**, 067210 (2001).
[6] J. Kreisel, G. Lucazeau, C. Dubourdieu, M. Rosina, and F. Weiss, J. Phys.: Condens. Matter **14**, 5201 (2002).
[7] T. Shibata, B. Bunker, J. F. Mitchell, and P. Schiffer, Phys. Rev. Lett. **88**, 207205 (2002).
[8] C. Renner, G. Aeppli, B. G. Kim, A. S. Yeong, and S. W. Cheong, Nature (London) **416**, 518 (2002).
[9] A. Moreo, S. Yunoki, and E. Dagotto, Science **283**, 2043 (1999).
[10] Y. Tokura and N. Nagaosa, Science **288**, 462 (2000).
[11] E. Cockayne and K. M. Rabe, Phys. Rev. **57**, 13 973 (1998).
[12] L. Bellaiche and D. Vanderbilt, Phys. Rev. Lett. **81**, 1318 (1998).
[13] J. Iniguez and L. Bellaiche, Phys. Rev. Lett. **87**, 095503 (2001).
[14] J. Kreisel, B. Dkhil, P. Bouvier, and J. M. Kiat, Phys. Rev. B **65**, 172101 (2002).
[15] J. Kreisel, A. M. Glazer, P. Bouvier, and G. Lucazeau, Phys. Rev. B **63**, 174106 (2001).
[16] I. Loa, P. Adler, A. Grzechnik, K. Syassen, U. Schwarz, M. Hanfland, G. K. Rozenberg, P. Gorodetsky, and M. P. Pasternak, Phys. Rev. Lett. **87**, 125501 (2001).
[17] J. S. Zhou and J. B. Goodenough, Phys. Rev. Lett. **89**, 087201 (2002).
[18] Y.-M. Chiang, G. W. Farrey, and A. N. Soukhojak, Appl. Phys. Lett. **73**, 3683 (1998).
[19] G. O. Jones and P. A. Thomas, Acta Crystallogr., Sect. B: Struct. Sci. **58**, 168 (2002).
[20] G. O. Jones, J. Kreisel, and P. A. Thomas, Powder Diffr. **17**, 301 (2002).
[21] S. Vakhrushev, A. Nabereznov, S. K. Sinha, Y. P. Feng, and T. Egami, J. Phys. Chem. Solids **57**, 1517 (1996).
[22] H. You and Q. M. Zhang, Phys. Rev. Lett. **79**, 3950 (1997).
[23] N. Takesue, Y. Fujii, M. Ichihara, and H. Chen, Phys. Rev. Lett. **82**, 3709 (1999).
[24] N. Takesue, Y. Fujii, and H. You, Phys. Rev. B **64**, 184112 (2001).
[25] In this paper we refer all indices to a doubled pseudocubic perovskite unit cell.
[26] A. M. Glazer, Acta Crystallogr., Sect. B: Struct. Crystallogr. Cryst. Chem. **28**, 3384 (1972).
[27] A. Guinier, *Théorie de la radiocristallographie* (Dunod, Paris, 1964).
[28] B. E. Warren, B. L. Averbach, and B. W. Roberts, J. Appl. Phys. **22**, 1493 (1951).
[29] T. R. Welberry, J. Appl. Crystallogr. **19**, 382 (1986).
[30] T. R. Welberry and B. D. Butler, J. Appl. Crystallogr. **27**, 205 (1994).
[31] G. O. Jones and P. A. Thomas, Acta Crystallogr., Sect. B: Struct. Sci. **56**, 426 (2000).
[32] B. Noheda, Curr. Opin. Solid State Mater. Sci. **6**, 27 (2002).
[33] B. Dkhil, J. M. Kiat, G. Calvarin, G. Baldinozzi, S. B. Vakhrushev, and E. Suard, Phys. Rev. B **65**, 024104 (2002).
[34] J. Kreisel, A. M. Glazer, G. Jones, P. A. Thomas, L. Abello, and G. Lucazeau, J. Phys.: Condens. Matter **12**, 3267 (2000).
[35] T. R. Welberry, R. L. Withers, and S. C. Mayo, J. Solid State Chem. **115**, 43 (1995).
[36] T. R. Welberry and A. G. Christy, Phys. Chem. Miner. **24**, 24 (1997).
[37] S. C. Mayo, T. Proffen, M. Bown, and T. R. Welberry, J. Appl. Crystallogr. **29**, 464 (1999).
[38] T. R. Welberry and S. C. Mayo, J. Appl. Crystallogr. **29**, 353 (1996).
[39] T. R. Welberry and A. M. Glazer, J. Appl. Crystallogr. **27**, 733 (1994).
[40] T. R. Welberry, T. Proffen, and M. Bown, Acta Crystallogr., Sect. A: Found. Crystallogr. **54**, 661 (1998).
[41] T. R. Welberry, D. J. Goossens, A. J. Edwards, and W. I. F. David, Acta Crystallogr., Sect. A: Found. Crystallogr. **57**, 101 (2001).
[42] T. R. Welberry and M. Honal, Z. Kristallogr. **217**, 422 (2002).
[43] G. O. Jones, in Ph.D. thesis, University of Warwick, Warwick, 2001.
[44] M. Geday, J. Kreisel, K. Roleder, and A. M. Glazer, J. Appl. Crystallogr. **33**, 909 (2000).
[45] I. G. Siny, C. S. Tu, and V. H. Schmidt, Phys. Rev. B **51**, 5659 (1995).
[46] W. Zhong and D. Vanderbilt, Phys. Rev. Lett. **74**, 2587 (1995).
[47] J. Iniguez and D. Vanderbilt, Phys. Rev. Lett. **89**, 115503 (2002).
[48] B. Chaabane, J. Kreisel, B. Dkhil, P. Bouvier, and M. Mezouar, Phys. Rev. Lett. **90**, 257601 (2003).